Received 18 July 2024; revised 29 August 2024; accepted 17 September 2024. Date of publication 25 September 2024; date of current version 7 October 2024.

Digital Object Identifier 10.1109/OJCOMS.2024.3467680

WiLO-OFDM Transmission Scheme for Simultaneous Wireless Information and Power Transfer

STEVEN CLAESSENS [1], PRERNA DHULL [1,2] (Graduate Student Member, IEEE), DOMINIQUE SCHREURS [1] (Fellow, IEEE), AND SOFIE POLLIN [1] (Senior Member, IEEE)

[1]Division WaveCoRE, Department of Electrical Engineering, KU Leuven, 3001 Leuven, Belgium

[2]RF and Communication Technologies Research Laboratory, University of Technology Sydney, Sydney, NSW 2007, Australia

CORRESPONDING AUTHOR: P. DHULL (e-mail: Prerna.Dhull@student.uts.edu.au)

This work was supported in part by the Flemish Fonds voor Wetenschappelijk Onderzoek âĂŞ Vlaanderen (FWO) Strategisch Basisonderzoek (SBO) loBaLeT (Sustainable Internet of Battery-Less Things) Project under Grant S001521N; in part by the (Massive Backscattering for High Throughput Zero Power Wireless Networking) Project under Grant FWO G085818N; and in part by the SUPERIOT Project through the Smart Networks and Services Joint Undertaking (SNS JU) under the European Union's Horizon Europe Research and Innovation Programme under Grant 101096021.

ABSTRACT Lowering the dependency of receivers and sensors on energy supplies is a requirement for a realistic Internet of Things. This is certainly achieved when sensor nodes are powered wirelessly. Local oscillators (LOs), required to receive and transmit modern radio frequency (RF) waveforms, consume a considerable amount of the power budget. We propose a Wireless Local Oscillator (WiLO) concept to move the LO from the sensor to an external location and transmit it wirelessly to the sensor. This WiLO is modeled as a constant tone transmission. As is well known, the sensor can backscatter the constant tone, which enables uplink transmission. Our system approach allows the downconversion of any RF waveform without LO and mixer while simultaneously utilizing the same signal for power transfer. In this work, we demonstrate our approach to different types of OFDM signals, which can be considered as a general complex RF signal example to be received. Our WiLO-based technique to receive any modern communication signal without LO, in combination with harvesting energy from the tone and backscattering on that tone, results in a promising energy-efficient IoT solution. We present the performance model with design requirements for WiLO tone and amplitudes of OFDM tones for feasible reception of WiLO-OFDM. Simultaneous Wireless Information and Power Transfer (SWIPT) applications typically operate in a high SNR regime, and both energy harvesting and information transfer are equally important. The cost of 12 dB performance with an AWGN noisy channel can be acceptable by saving a significant amount of power by removing the LO.

INDEX TERMS Energy harvesting, envelope detector, Internet of Things (IoT), local oscillator, OFDM, receiver architecture, simultaneous wireless information and power transfer (SWIPT).

I. INTRODUCTION

THE WORLD of the Internet of Things (IoT) promises the deployment of many sensors and products in our environment. Lowering the battery dependency of those nodes is a requirement for realistic IoT implementations. A promising solution to reduce battery dependence is simultaneous wireless information and power transfer (SWIPT), where the communication signal used for information transmission is also used for simultaneous power transfer, utilizing the resources more efficiently.

Till now, most of SWIPT research revolved around separated information and energy receiver architectures where separate modules are used to process information decoding and power transfer at receiver [1], [2]. The received signal is split into two separate paths at receiver front, one for information decoding and the other for energy harvesting. In

such cases, the rectifier is solely used for energy harvesting, and conventional information receivers perform information decoding. High-frequency radio frequency (RF) components used in conventional information receivers consume a high amount of power. For example, the power consumption of a full ultra-low-power receiver is 3.8 mW, out of which 28% of total power consumption is consumed by the local oscillator (LO), and 9% is consumed by a mixer [3], [4]. An RF LO needs to maintain stability and low power noise while operating at high frequencies, resulting in an overall high-power consumption.

Recently, an idea of utilizing a rectifier for dual purpose, both energy as well as information decoding, has been introduced to remove the power-consuming LO-mixer topology and reduce the circuit complexity, making it more suitable for simple IoT nodes [5], [6], [7]. However, it is not possible to use conventional modulation schemes for information transmission for information detection via only a rectifier at the receiver. Therefore, new modulation techniques need to be developed so that information decoding and power transfer can be performed on the same signal simultaneously.

This work proposes the transmission of a wireless local oscillator (WiLO), which is a continuous waveform (CW), to enable a collection of techniques for energy-efficient IoT systems. This set of techniques comprises energy harvesting, backscatter transmissions, and the reception of any modern communication signal without a local oscillator at the sensor. Information is decoded from the rectifier output signal by exploiting the non-linearity of the rectifier while simultaneously using the same rectified signal for energy harvesting. This eliminates the need for a local oscillator and mixer, reducing the form factor for the receiver and lowering the power consumption on board.

A. LITERATURE AND MOTIVATION

Energy harvesting, uplink backscattering, and downlink LO-less downconversion techniques cover the necessary functions of low-power and energy-efficient IoT networks. The transmission of WiLO tone, in addition to OFDM information data, provides the advantage of using the same communication signal for both information transfer and power transfer using only a rectifier.

Any sensor can harvest energy from wireless signals using rectifier hardware. The availability of a constant tone at the sensor antenna is also ideal for backscatter communications. Classically, sensors require an LO to upconvert its communication signal for transmission. Recently, prominent research has been performed on backscatter-communication-based green IoT [8]. With backscattering, however, the received high-frequency tone is reflected back in a modulated way without LO. Backscatter research has shown that not only basic amplitude modulations, which vary the level of reflection, are possible, but also QAM, PSK, and even Bluetooth signal can be created for uplink communication [9], [10], [11], [12]. Backscatter communication techniques: threshold comparison and feature extraction do not utilize the non-linearity of the rectifier for downlink information decoding without LO [13]. Therefore, a constant WiLO tone with the information data can provide a solution for both SWIPT and backscatter communication.

A vast amount of research has been conducted for SWIPT with separated information and energy receiver architecture where the received signal is split for information path and energy path with the help of power splitting, frequency splitting, or time-switching at the receiver input [1], [14], [15], [16]. Here, conventional methods are used for information decoding consisting of LO-mixer topology consuming a significant amount of power for signal processing [3], [4]. Therefore, integrated information-energy SWIPT architecture has been introduced [5]. However, for integrated information-energy SWIPT architectures, new communication techniques need to be developed for an integrated reception of power and information at the rectifier output.

Much research has been conducted to improve the rectifier's power conversion efficiency (PCE) [17]. Due to the rectifier's non-linearity, the rectified DC power at the output is not only a function of rectenna design and received signal strength but also a function of the shape of the received waveform [18], [19], [20]. It has been shown that the PCE of the rectifier can be increased by having a high peak-to-average power ratio (PAPR) at the rectifier input [18], [21], [22]. Impact of multitone waveforms and rectifier design with their several parameters such as transmitted power, frequency spacing, rectifier's low-pass-filter cut-off frequency, etc., have been studied intensively [23], [24], [25], [26].

The diode's intermodulation process is already known for a long time [27]. This is both inconvenient and useful at the same time. On one hand, the resulting baseband tones are superpositions of different intermodulation products (IMs) of the RF input tones, which implies distortion of the information and loss of frequency orthogonality. On the other hand, this intermodulation process downconverts the signal without the need for a power-consuming local oscillator-mixer topology. Hence, with some design guidelines for the WiLO tone, the information can be retrieved from the diode's intermodulation products, and sufficient frequency orthogonality can be obtained for any type of information signal without requiring a power-consuming LO-mixer topology.

Concerning using this technique in SWIPT systems, classical OFDM as a high PAPR signal for pure wireless power transfer (WPT) has been studied in [18]. The authors of [21] proposed a superposition of a multitone signal for WPT and a low-power OFDM signal for wireless information transfer (WIT). A selective OFDM approach using the redundant cyclic prefix for power transfer with negligible impact on information transfer for a time-switching receiver is proposed in [28], [29]. Here, some portion of the OFDM information symbol is also utilized for energy harvesting in addition to the redundant cyclic prefix, although this quickly results in a decreased information rate. As a result, the

length of this information part used for energy harvesting is optimized according to the energy requirement at the receiver. In addition to the time-switching assumption, a separated information-energy receiver architecture is used in this work, and neither addresses how the OFDM signal's information can be received by small wirelessly powered sensors consisting of a simple rectifier destroying orthogonality between subcarriers.

A simple SWIPT transmission scheme using different energy levels of a single-tone signal is introduced where different energy levels correspond to different amplitude symbols while simultaneously receiving the power through the same rectifier-receiver circuitry [5]. Further, a biased-ASK transmission scheme for rectifier-receiver architecture is introduced where each amplitude symbol is allocated some minimum energy level to ensure a continuous power transmission at the receiver [30]. However, in these schemes, the much more complex case of OFDM, where multiple symbols over multiple tones are transmitted, is not considered, and only a single tone is utilized.

The idea of using multiple tones is introduced in [31] where information is embedded in the ratio of tones' amplitude for reducing the effect of transmission distance. However, it has been shown that the complexity of information detection increases as the number of tones increases. Another information transmission method utilizing a multitone signal for its enhanced WPT efficiency is introduced in [32] where different symbols are transmitted by varying the number of tones in the transmitted multitone signal, resulting in different PAPR levels at the output as PAPR $\propto 2N$. However, distinct symbols result in unequal multitone signal bandwidths requiring a large bandwidth for input matching network. Furthermore, a 2-D transmission scheme based upon the subcarriers-number component and the subcarriers-amplitudes is introduced [33]. PAPR value is used to decode subcarriers-number component and the rectifier output current intensity is used to decode subcarriers-amplitudes.

A frequency-based multitone transmission scheme multitone FSK where information is embedded through the transmitted multitone frequency spacing and fast Fourier transform (FFT) is used for information detection at receiver [34]. However, only one symbol is transmitted per multitone signal transmission, and OFDM-type communication is not feasible. In [35], a phase-based multitone transmission scheme has been introduced where it is possible to transmit multiple symbols over a multitone stream while simultaneously utilizing the signal for WPT with the same rectifier circuitry. However, phase synchronization becomes critical in this case.

The receiver topologies presented in [6], [36], demonstrate the successful reception of a single carrier information signal with a remote local oscillator, such as a single Bluetooth channel ([36]) or a carrier modulated with 802.15.4 direct sequence spread spectrum signal ([6]). While similar and practical, both require large spacing between information signal and continuous tone, relative to the information bandwidth, and neither considers the impact of WiLO amplitude, phase, and frequency offset tuning, which is required for LO-less multicarrier information signal downconversion as outlined in this work, lacking generality to more complex signals of those methods. Existing transmission methods for SWIPT have been summarized in Table 1.

As a solution, we introduced a novel technique in [37] illustrated by modifying an ASK-OFDM modulated signal so it can be received without an LO. A simple envelope detector or rectifier circuit is able to receive ASK-OFDM by solely adding one extra tone to the original modulated signal, relying on the diode's non-linear behavior. Recently, other communication techniques optimized for SWIPT have been introduced, which enable efficient energy harvesting while being able to be downconverted by the same rectifier hardware, enabling integrated receivers for SWIPT [30], [31], [34]. However, the possibility of an OFDM-type communication has not yet been explored, where multiple symbol transmission is possible with only a single waveform transmission.

Although the usage of a rectifier for information downconversion removes the frequency orthogonality at the rectifier output, it is possible to attain sufficient orthogonality for information detection from baseband tones at the rectifier output, with the help of proper design guidelines for WiLO tone and OFDM information data. The main innovation in our work is hence two-fold: (a) we don't rely on time-switching and achieve truly simultaneous information and energy transfer, and (b) we reuse the same hardware as the rectifier is taking care of the translation of the passband RF signal to baseband. The OFDM waveform is designed to achieve such rectifier-based information and energy reception at the same time.

B. CONTRIBUTIONS

This paper discusses the LO-less downconversion more in-depth, demonstrating that any modern communication signal can be downconverted when it is received together with a constant tone, a WiLO, by a sensor with an envelope detector or a simple rectifier hardware. Hence, no local oscillator is required to translate the received RF signal to the baseband. This modified OFDM scheme is defined as WiLO-OFDM since the technique comprises adding a constant tone, the WiLO, to the signal spectrum of an OFDM modulated signal. The main contributions of this paper are summarized below:

- By transmitting only one extra constant pilot tone (WiLO) together as a reference with the signal, information can be decoded from second-order intermodulation products (IM_2) of the rectified baseband signal by utilizing its non-linearity while simultaneously receiving the power from the same signal. The proposed technique is illustrated in the frequency domain.
- While the integrated receiver destroys the orthogonality of the baseband IM_2 signals, we show that the WiLO

TABLE 1. Summary of existing transmission methods for SWIPT.

Ref.	Transmission Approach	Receiver Architecture	Characteristics
[21]	Superposition of multitone signal over OFDM signal	Separated	- Superposition of a multitone signal for WPT and a low-power OFDM signal for WIT. - Saturation of ADC may occur. - For information detection, cancellation of the power signal is required. - $1.8\,\mu$A for SNR $=20$ dB and 1 bit/s/Hz.
[28], [29]	Selective OFDM approach	Separated	- Cyclic prefix and some portion of the information part is utilized for energy harvesting. - Linear energy harvester model is used. - $\sim$38% PCE for SNR $=20$ dB and 2 bits/subcarrier channel.
[5]	Energy modulation	Integrated	- Single tone signal is used. - Different energy levels correspond to different amplitude symbols. - Not taking advantage of multitone carriers to enhance the power transfer.
[30]	Biased-ASK	Integrated	- Some minimum energy level is allocated to each amplitude symbol to ensure a continuous power transmission at the receiver. - Single tone signal is used. - OFDM type multiple symbols transmission is not possible. - 0.13 V and BER of 10^{-4} for $A_{\text{ratio}}=0.5$, SNR $=18$ dB at -20 dBm received power.
[31]	Ratio ASK	Integrated	- Multitone signal is used. - Information is embedded in the ratio of tones' amplitudes. - The complexity of information detection increases as the number of tones increases by more than two. - 48% PCE for two tones signal with power ratio of $1/6$ for received power of -10 dBm.
[32]	PAPR based	Integrated	- Different multitone PAPR levels correspond to different symbols at the output. - Equal tone spacings result in unequal signal bandwidths for the distinct symbols. - A large bandwidth input matching network is required and performs well only for high SNR. - For an input power of -10 dB, BER $=10^{-1}$ and $0.5\,\mu$A.
[34]	Multitone-FSK	Integrated	- Information is embedded through the transmitted multitone frequency spacings. - Lower envelope variations. - Only one symbol per transmission and no OFDM-type communication. - For 0 dBm received power, 0.55 V and SER $=10^{-2}$.
[35]	Multitone PSK	Integrated	- Information is embedded in the tones' phases of a multitone signal. - Lower envelope variations. - Maintaining phase synchronization is challenging. - PCE $=\sim 40\%$ and BER $=0.047$ for a received input power of -6 dBm.
[6], [36]	Single Bluetooth channel	Local oscillator	- Single carrier information signal is used. - Large spacing between information signal and continuous tone relative to the information bandwidth. - The impact of WiLO amplitude, phase, and frequency offset tuning is not considered. - -40 dBm for a 10 dBm Bluetooth low energy source at $2\,\mathrm{m}$ distance.
	Proposed WiLO-OFDM	Integrated	- Multitone signal is used. - Multiple symbols per waveform transmission and OFDM-type communication. - Modern communication signals WiLO-ASK-OFDM, WiLO-PSK-OFDM, and WiLO-QAM-OFDM can be received for SWIPT. - Design guidelines for WiLO tones and maximal amplitudes of OFDM tones exist for feasible information detection. - Constant WiLO-tone can be located very close to the information spectrum, resulting in an increased spectral efficiency. - BER $<10^{-3}$ for $N=4$, $M=4$ WiLO-ASK-OFDM with $r=0.35$ at 10 dB SNR.

amplitude can be controlled to achieve sufficient orthogonality. An upper limit for the ratio between WiLO tone and the maximal amplitudes of OFDM tones r_{u} is studied till where sufficient orthogonality is obtained and OFDM can be achieved with the WiLO receiver.

- A performance model for WiLO-ASK-OFDM is provided by analyzing various waveform designing parameters with mathematical, simulation, and measurement-based analysis. For feasible information decoding from IM_2s, design guidelines for OFDM,

operable amplitudes of tones, and WiLO design are studied. An upper limit on amplitudes of information tones is demonstrated, making the detection possible by neglecting non-orthogonal non-linear distortion and the combined effect with WiLO phase optimization over waveform PAPR is analyzed.
- WiLO-ASK-OFDM is extended to PSK and QAM modulated OFDM and validated by simulations and measurements. It is shown that both amplitude and phase information from the different tones can be recovered. The impact of the frequency spacing between the information signal and the constant tone and an Additive White Gaussian noise channel (AWGN) channel is analyzed.

C. PAPER OUTLINE

Transmitted signal design with WiLO design exploiting the non-linearity of the rectifier is introduced in Section II and a performance model for WiLO-ASK-OFDM is given in Section III. Next, it is extended to any modulation including phase modulated OFDM in Section IV and validated by simulations and measurements. The impact on the signal's PAPR is also studied as it is important for wireless power transfer. The impact of the frequency spacing between the information signal and the constant tone is characterized in Section V. Moreover, the impact of an AWGN channel is studied in Section VI. Finally, Section VII briefly discusses the integration of all WiLO subsystems, followed by the conclusions in Section VIII.

D. MATHEMATICAL, SIMULATION, AND EXPERIMENTAL MODEL

This work uses a simplified mathematical model, a simulation model, and an experimental setup to demonstrate how the described signal energy harvesting and reception method can replace a classical LO-mixer information receiver topology with a passive diode topology that enables simultaneous and integrated energy reception and information processing. The initial mathematical model that describes the mechanism behind the proposed technique is a simplified diode model with a focus only on IM_2, as baseband information is decoded using IM_2 baseband components of the received signal. Then, a simulation model (in MATLAB) is used to validate the mathematical results with a more realistic highly non-linear diode, implemented as a zero-threshold diode. Finally, experimental results with a practical rectifier are used to validate the feasibility in practice. The experimental setup is described in [37] and comprises a software-defined vector signal transceiver connected to the class-F rectifier described in detail in [38].

II. PROPOSED SIGNAL MODIFICATION

The proposed LO-less receiver technique comprises adding one constant tone to the spectrum of a modulated and upconverted baseband signal with spectrum $S_{\text{bb}}(f)$. The presence of the constant tone next to the information spectrum allows a receiver to downconvert the signal with a passive diode. It is important to note that contrary to DCO- and ACO-OFDM signals, the time domain baseband signal $s_{\text{bb}}(t)$ can be complex and does not need to be Hermitian symmetric.

A. TRANSMITTED SIGNAL

Our approach consists of adding only one constant tone, defined as the wireless local oscillator (WiLO), with an amplitude A and phase β next to the information signal spectrum in the frequency domain. This WiLO's frequency separation from the information signal can generally take any value, and the WiLO can be located at higher or lower frequencies than the information signal. In this work, the WiLO is located at lower frequencies, and the frequency separation with the information spectrum is defined as $c\Delta f$ with $2c$, an integer. We allow $c = 0.5$ in order to compare it with an RF adaptation of ACO-OFDM in Section V while generally limiting c to integer values to limit the impact on throughput because of the granularity of the Fourier transformation in the receiver. While it is not a requirement for the technique, the explanation in this work assumes that the signal is a collection of tones with frequency spacing Δf, with $f_n = n \times \Delta f$ for $1 \leq n \leq N-1$. Any information signal can be approximated by such a signal by taking a Fast Fourier transformation (FFT). Unless mentioned otherwise, we assume by default that the WiLO has a frequency $f_{\text{WiLO}} = f_{\text{inf,RF}}|_{\text{min}} - c\Delta f$, and unless specified otherwise $c = 1$ in this work, with $f_{\text{inf,RF}}|_{\text{min}}$ the lowest frequency tone in the information spectrum.

While the WiLO and the information signals can be transmitted by different transmitters and combined at the receiver antenna, for simplicity, we assume here that this tone is transmitted by the information transmitter, modifying the RF signal's single-sided spectrum to

$$\begin{aligned} S^{+}_{\text{rf}}(f) &= P\Big(Ae^{j\beta}\delta(f-(f_c-(c-1)\Delta f))\Big) \\ &\quad + P(S_{\text{bb}}(f-f_c)), \\ &= P\Big(Ae^{j\beta}\delta(f-f_c)\Big) \\ &\quad + P\left(\sum_{n=1}^{N-1} a_n\delta(f-(f_c+f_n))\right), \end{aligned} \tag{1}$$

with f_c the carrier frequency, a_n the complex coefficient of the tone on frequency f_n, S_{bb} the baseband signal in frequency domain, $Ae^{j\beta}$ the complex scaling factor for the WiLO, and P some power scaling value.

B. DIODE MODEL

The receiver contains a non-linear diode. So, next to harmonics at multiples of the carrier frequency f_c, the envelope detector's diode will also create intermodulation products at different frequencies both in RF and baseband. The receiver's low pass filter removes the high-frequency components, and our technique allows us to recover the information from the baseband intermodulation products.

The exponential non-linear behavior of the diode can be approximated by a Taylor model. This expression reveals the different baseband components at the diode's output due to different intermodulation orders. When, for example, the input of the diode is assumed to be a two-tone input signal, the Taylor term representing the baseband IM_2, which we assume to be dominant in the baseband, can be modeled by

$$IM_2 = k \times A_1 A_2 \cos(2\pi t(f_1 - f_2) + (\phi_1 - \phi_2) + \phi), \quad (2)$$

with A_1 and A_2 the amplitudes, f_1 and f_2 the frequencies, and ϕ_1 and ϕ_2 the phases of the first and second input tones, respectively. Factor k represents the amplitude scaling and ϕ is the phase shift caused by the diode. Eq. (2) shows that the following three basic properties of IM_2 are:

- the frequency of IM_2 equals the frequency spacing between the two intermodulating tones,
- the amplitude of IM_2 relates to the product of the two intermodulating tones' amplitudes,
- the phase of IM_2 relates to the phase difference between the two intermodulating tones.

These IM_2 properties have been used recently in designing SWIPT modulation techniques [31], [39]. In these works, the intermodulation effect on a multitone signal is modeled as a superposition of multiple two-tone intermodulations. Hence, the spectrum $S_{rf}(f)$ with N tones, described by (1), has $N(N-1)/2$ different tone pairs, creating $N(N-1)/2$ second order intermodulation contributions at $N-1$ unique baseband frequencies. This is because the closest pair of tones has frequency spacing Δf, and the farthest pair of tones has frequency spacing $(N-1)\Delta f$. We assume that the low pass filter removes higher-frequency components. Since the rectifier baseband output signal created by this intermodulation mechanism, is not dependent on the original signal frequencies but on the frequency difference $c\Delta f$ between the WiLO and the information signal, $S_{rf}(f)$ in (1) can be shifted and centered around some carrier frequency f_c without any impact on our proposed technique, similar to multitone FSK [39].

C. WILO DESIGN

Throughout this work, the WiLO amplitude A is normalized to one and the information signal is scaled as the amplitude ratio between the maximal amplitude of the information tones ($|a_{n,M-1}|_{\max}$), so $A = |a_{n,M-1}|_{\max}/r$.

The design rules in this work limit the maximal information tone amplitude r to r_u, for the technique to work as outlined next.

1) BALANCING INTERMODULATION CONTRIBUTIONS

Two types of diode output intermodulations are defined:

- inter-intermodulations (inter-IM): the baseband second-order intermodulations between each information tone and the WiLO
- intra-intermodulations (intra-IM): the baseband second order intermodulations among information tones

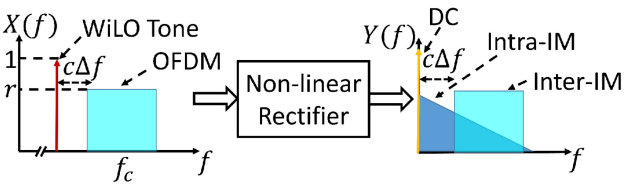

FIGURE 1. Input spectrum $X(f)$ and output spectrum $Y(f)$ of the proposed signal design, demonstrating the inter-(light) and intra-(dark) second-order intermodulation products in baseband.

So, since the intermodulation product amplitudes in (2) relate to the amplitudes of the input tones, the inter-IM scale with r whereas the intra-IM among information tones scale with r^2. The upper limit on maximal signal tone amplitude r, r_u, that still results in decodable baseband components at the diode output turns out to be dependent on the information signal's modulation scheme, the number of tones, and the WiLO's phase offset β.

Fig. 1 shows the general principle of adding a WiLO tone to a general signal spectrum to create useful IM_2's in baseband after passing a non-linear system. It can be seen that both power and information are extracted from the same signal simultaneously. Intra-IMs are the result of intermodulation between WiLO tone and information tones whereas Inter-IMs are intermodulations among information tones. The required information is present in the Intra-IMs. It is clear from the figure that increasing c lowers the overlap between the inter- and intra-intermodulations, at the cost of spectral efficiency. Each set of $N-1$ information tones and a WiLO at the diode's input corresponds to a unique set of $N-1$ tone amplitudes at the diode output. For classical OFDM where the tones are fully orthogonal, modulated tones can be recovered at the receiver after LO-based downconversion and the FFT operation. However, in this case, with a diode-based receiver, each frequency bin of the diode baseband output consists of IM_2 components from a large subset of modulated subcarriers. For example, the baseband tone at $f = c\Delta f$ contains the intermodulation between the first information tone and the WiLO but also all the second-order intermodulations between other information tone pairs with frequency spacing $c\Delta f$.

2) OPERABLE r

At $r = r_u$, output constellations are nearly inseparable. For $r < r_u$, the error vector magnitude decreases, and the information transfer becomes more robust to noise. This is illustrated in Fig. 2 for 5-tone ASK-OFDM for a low r of 0.01 and $r \approx r_u$ of 0.15 where the distinction between symbols becomes difficult for the latter case. For 5-tone signal and $c = 1$, the required information would be at inter-IMs at Δf, $2\Delta f$, $3\Delta f$, $4\Delta f$, and $5\Delta f$. Amplitudes of these IM_2s is a result of the product of WiLO tone amplitude A and information tone's amplitude r, i.e., $A.r = r$ from (2) for $A = 1$. Similarly, the interfering IM_2s (Intra-IM) amplitudes are proportional to r^2. As r increases, the influence of these Intra-IMs over desired Inter-IMs increases and results

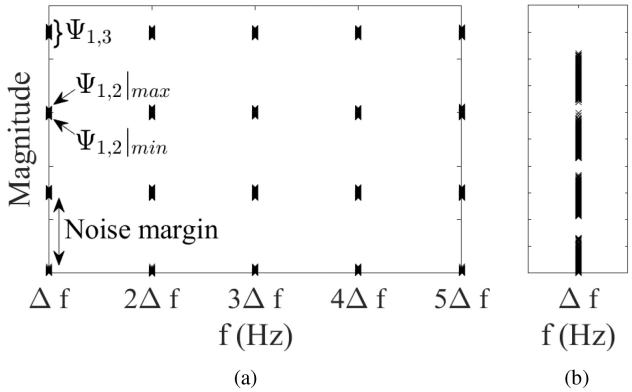

FIGURE 2. Baseband diode output for WiLO and 5-tone ASK-OFDM with $M = 4$ and $c = 1$ input signal without noise, when (a) $r = 0.01$ and (b) $r = 0.15$.

in a significant distortion. Fig. 2 highlights this increased distortion with increasing r from 0.01 to 0.15. To balance out these unnecessary Intra-IMs from the desired Inter-IM, WiLO amplitude A is kept strong enough.

This figure clearly shows that the 5-tone ASK-OFDM signal can be recovered from the diode baseband output. $\psi_{n,m}$ is the collection of outputs on tone n with frequency $f = (c + n - 1)\Delta f$ in the baseband output, for input tone symbol $a_{n,m}$ with index m, on the n-th information tone.

When not restricting maximal information tone amplitudes (r) to some r_u, and $r > r_\mathrm{u}$, the baseband outputs $\psi_{n,m}$ on tone n are not easy to separate and demap. So, the WiLO has to be designed strong enough ($r \leq r_\mathrm{u}$) such that from each baseband tone at $f_n = (c + n - 1)\Delta f$, $\psi_{n,m}$ do not overlap for different input symbol index m.

3) RECEIVER METHODS

Since the input-output relation of the diode remains deterministic, it would be possible to nearly completely remove the WiLO and design the signal with large r when demapping the FFT output tone constellations with a look-up table. However, the number of pairwise intermodulation combinations, each generating an additional unique output, rapidly increases with M^{N-1}, which makes this approach unfeasible for reasonable N in an IoT application, concerning memory and processing limitations. Also, while a look-up table detection would theoretically work, such distorted constellations would be extremely sensitive to noise. Simulations for signals without limited r_u and very distorted output constellations could still be demodulated successfully with for example Long Short-Term Memory (LSTM) deep learning [40], [41], but those results are omitted in this work because of the aforementioned reasons. In this work, the receiver processing is kept flexible with regards to automatically coping with diode amplitude distortion and phase shift by using shallow machine learning based on support vector machines (SVM) to easily demap information from clear output constellations. However, this is not required for the technique to work and classical detection processing can be used, but feasible r_u will slightly decrease because of the unconventional received symbol's distribution as shown in Fig. 4.

4) DESIGN GUIDELINE FOR OFDM

The challenge in using this WiLO approach as an alternative for the receiver LO is finding the WiLO amplitude A and phase β (and tone spacing c) in (1) that balance the useful and interfering intermodulation products created by the diode, to obtain demappable output constellations. The receiver also has to account for the diode's shifting amplitude and phase of the signal. A theoretical model as well as simulation and experimental-based solutions for finding both A and β, are discussed next for different types of OFDM signals with $N - 1$ tones, frequency spacing Δf, and the same type of modulation on each tone. The modulation technique, the number of information tones as well as the WiLO frequency spacing have an impact on A and β.

5) IMPACT OF NOISE ON OPERABLE r

Another motivation for maximizing r, which means minimizing WiLO amplitude A, is optimizing throughput for a certain amount of tones and bandwidth. For example, in the presence of noise, as discussed in Section VI, it is beneficial to have strong information tones with high r. Choosing for maximal $r = r_\mathrm{u}$, however, does not maximize throughput since the signal would be extremely sensitive to noise because of the intra-IM products already filling the noise margin as shown in Fig. 2. The optimal r, r_o when throughput is maximal, is lower: high enough to provide a high information signal-to-noise power ratio but low enough compared to maximal r to have enough noise margin to cope with the noise present. Hence, a modulation scheme that results in higher r_u is a good strategy since it allows r_o to increase also. What optimal r (r_o) is and how it relates to maximal r (r_u) is shown in Section VI where the impact of an Additive White Gaussian noise channel (AWGN) is studied. The upper limit of r, for which information transfer is still possible is defined as $0 \leq r_\mathrm{u}$. Optimal r that maximizes throughput in the presence of noise is defined as $0 \leq r_\mathrm{o} \leq r_\mathrm{u}$.

6) THREE TYPES OF INTERFERENCE

The baseband second-order intermodulations between each information tone and the WiLO (inter-IM), are useful, while the baseband second-order intermodulations among information tones (intra-IM), create interference. Three types of interference are identified.

- Additive second-order interference, as any pair of tones with the same frequency spacing, creates second-order intermodulations at the same baseband frequency. Hence, different IM_2s superpose whereas only one of them is useful.
- Additive higher-order interference, as higher even order modulations are also located in baseband and can also add up and interfere with the useful intermodulation products, similar to the previous interference type.
- Power interference, as the intermodulation strength is impacted by conservation of power. A tone's intermodulation with the WiLO is stronger if no other

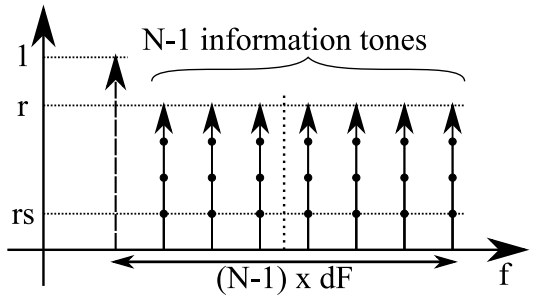

FIGURE 3. Frequency domain constellation of the biased ASK modulated version of the proposed OFDM signal, with $N-1=7$ information tones and modulation order $M=4$ per tone [37].

tones with which it also intermodulates are present at the diode input. Hence, the useful intermodulations themselves are modulated by the number and strength of the other present tones and the power that is lost in intermodulations with those.

The mathematical model in this work only accounts for the first type of interference as it is the strongest in the proposed operating range for $c\Delta f$. Power interference becomes prominent when the frequency spacing between the WiLO and the information spectrum, $c\Delta f$, is increased, as discussed in Section V.

In the next section, we further investigate receiving such a modified OFDM signal when assuming a (biased) ASK modulation (bASK) on the $N-1$ information tones. Parameters guidelines A and β are found while maximizing r in order to minimize the amount of power lost in the WiLO relative to the information signal. The technique is illustrated for PSK- and QAM-OFDM in Section IV.

III. MODIFIED BIASED ASK-OFDM MODULATION

In this section, the $N-1$ information tones are ASK modulated. A biased version of ASK (bASK) is utilized, in which the minimum amplitude is not zero but some ratio s of the maximal amplitude in the information tone's constellation [30], [42]. Such a bASK-OFDM signal in combination with the WiLO is shown in Fig. 3. Each of the information tones has an independent amplitude level between $r\times s\geq 0$ and r when normalizing (and fixing) the amplitude of the WiLO to 1. s is the ratio of the minimum available amplitude of the symbol to the maximum available amplitude of the symbol. For now, the channel is assumed noiseless whereas the AWGN channel impact is discussed in Section VI.

Using the biased ASK from [30] and maximal amplitude level r, we assume that each tone is modulated using the same M possible values, resulting then in $(N-1)^M$ possible OFDM symbols. For biased ASK, the following amplitudes are possible on each tone n

$$A_{n,m}\in\left\{r\left(\frac{1-s}{M-1}m+s\right)|m=0,\ldots,M-1\right\}, \tag{3}$$

with modulation order M, r the scaling factor of the maximal amplitude and the WiLO, and s the amplitude ratio of the individual tone's biased ASK modulation between minimal and maximal amplitude. We note $A_{n,m}$ if the amplitude on tone n equals the m-th value in that set, e.g., the value of $A_{n,M-1}=r$, which is expected as the WiLO magnitude is normalized to one. Both r and s are amplitude ratios, bound by $0\leq s<1$ and $0<r<r_{\mathrm{u}}$. For ASK modulated tones, the outputs ψ_n also resemble ASK constellations. Limiting r to r_{u} ensures that the output tone symbols $\psi_{n,m}$ for input tone symbol $a_{n,m}$, do not overlap with the output amplitudes $\psi_{n,i\neq m}$ from another input symbol, as shown in Fig. 2.

When the signal with N tones is applied at the diode's input, the frequency component at $f=(c+n-1)\Delta f$ has $N-n$ second order contributions, with $1\leq n\leq N-1$. Hence, the first second-order intermodulation product at $f=c\Delta f$ is assumed to contain the most interference in this model. Higher order intermodulation products in baseband, located at multiples of the frequency spacing, also cause interference but are smaller in amplitude. This is why the following mathematical analysis to find r_{u} is based on the quality of the information in the first information tone ($n=1$), received at $f=c\Delta f$ in the rectifier output signal spectrum.

A. MATHEMATICAL MODEL FOR WILO-BASK-OFDM

To avoid demodulation errors, since multiple intermodulation products may accumulate on each of the baseband frequency bins, the upper limit on r, r_{u}, is found assuming that the output at $f=c\Delta f$ in the output spectrum of the envelope detector, ψ_1, contains most interference. r_{u} is then the scaling factor that ensures no overlap between the $\psi_{1,m}$ after the channel and non-linear detector.

$\psi_{n,m}|_{\min}$ and $\psi_{n,m}|_{\max}$ indicate the minimal and maximal output tone's amplitudes for corresponding input tone amplitude $A_{n,m}$ as shown in Fig. 2.

In order to receive all information and to easily demap the constellation correctly, $\psi_{n,m}$'s on tone n should not overlap as motivated at the start of this section. This is expressed for the bASK-OFDM case by demanding that $\psi_{n,m}|_{\min}$ is larger than the largest output for a neighboring input tone symbol with a smaller amplitude ($\psi_{n,m-1}|_{\max}$), for every $1\leq m\leq M-1$. This results in

$$\psi_{n,m}|_{\min}>\psi_{n,m-1}|_{\max},\ \text{for}\ 1\leq m\leq M-1. \tag{4}$$

Outputs ψ_n depend on the interference by the other input signal tones and on the nonlinear characteristics of the envelope detector's diode. This section mathematical model assumes that interference is minimized or maximized by assuming minimal or maximal amplitudes for the other information tones, respectively, since the interference is related to amplitude products and scaled by a factor k in our IM_2 model, as shown with (2).

Each element in $\psi_{1,m}$ contains three second-order IM contributions: the useful second-order intermodulation between the first information tone (with $a_{1,m}$) and the WiLO, the second-order intermodulation between the first ($a_{1,m}$) and

second ($a_{2,m}$) information tone, and the second-order intermodulations between all other pairs of neighboring tones. As mentioned before, higher-order intermodulation tones are ignored in this mathematical analysis, but accounted for in the simulations and experiments in this work. The first two contributions depend on the actual amplitude of the first tone, $A_{1,m}$. So, $\psi_{1,m}|_{\min}$ and $\psi_{1,m-1}|_{\max}$ are found assuming minimal and maximal amplitudes for all other tones, respectively, expressed by (5) and (6), shown at the bottom of the page, respectively, considering here $1 \leq m \leq M-1$.

Each pair of consecutive outputs ($\psi_{1,m}$,$\psi_{1,m-1}$) could lead to an upper limit for r, r_{u}. Using (4), (5), and (6):

$$r < \frac{1}{m-1+s(M-m-1)+(N-3)(1+s)(M-1)}. \quad (7)$$

r is minimized by setting $m = M-1$ in (7), which means that for the first tone, the outputs ψ_1 to amplitudes $A_{1,M-2}$ and $A_{1,M-1}$ are the first to overlap, leading to the following upper limit on r, r_{u}

$$r < r_{\mathrm{u}} = \frac{1}{(M-2)+(N-3)(1+s)(M-1)}, \quad \text{for } N \geq 3. \quad (8)$$

A simplified second-order intermodulation mechanism is used in this work to construct a coarse mathematical model in order to comprehend theoretically the interaction between the proposed signals and the envelope detector. As explained in Section II-C, only additive second-order interference is considered in this model. Constructing a fully accurate mathematical communication receiver model is not trivial because of the diode's non-linear behavior.

So, simulations are used to verify the mathematical results based on this limited model, to find parameter values, and to assess the performance of the proposed technique. For simulations, the diode is modeled using a zero-threshold switch, which can be considered the ideal diode. It is followed by a low pass filter with cut-off frequency f_{cut}, which is an approach commonly used in communication theory. The spectrum of the envelope detector output signal is obtained using an FFT, after which it is processed. This signal processing consists of clustering and classifying the received constellation on each of the $N-1$ baseband tones, mapping $\psi_{n,m}$ back to $a_{n,m}$. Even when assuming a noiseless flat channel, some interference because of other intermodulation products will be present in this system. By controlling A and β from (1), this interference and its impact are controlled as derived in (8). However, increasing r_{u} as much as possible by accurate clustering remains a non-trivial challenge in this diode-based non-linear receiver. Fig. 4 shows the shape of the received constellations on the first IM_2 in baseband for a bASK modulated multitone signal with $s = 0$, $r = 0.3$, $N = 6$, $M = 8$ and $\beta = \pi/2$, as well as the SVM decision regions.

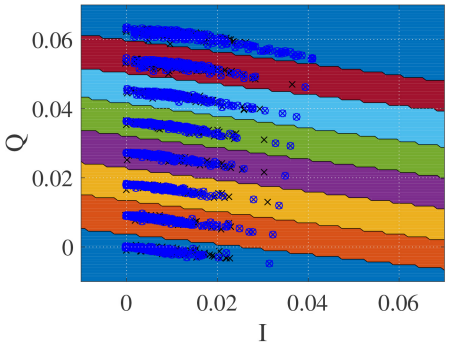

FIGURE 4. Simulated output response constellation for bASK with $s = 0$, $r = 0.3$, $N = 6$, $M = 8$, and $\beta = \pi/2$, with indicated SVM determined decision regions in different background colors and used samples for training indicated by blue circles.

Using the simulation model, the upper information tone amplitude limit r_{u} is found by varying modulation order M, the number of tones N, and r while verifying whether the clusters $\psi_{n,m}$ shown in Fig. 2 for different amplitudes overlap, according to (4), on any tone. r_{u} is shown in Fig. 5 (cross) as well as the mathematical result from (8) (circle). The simulation results match very well with the mathematical model when the latter is multiplied with a factor of 1.6. Both simulation results show that the upper limit on r decreases with both the modulation order M and the number of tones N. Without a model scaling factor, the mathematical model provides correct trends for the impact of M and N, while it is only an underlimit for r_{u}.

Regarding the mathematical model inaccuracy and required scaling, in practice, an input tone intermodulates with all other input tones, which lowers the strength of the

$$\begin{aligned}\psi_{1,m}|_{\min} &= k\left[A_{1,m} + A_{1,m}A_{2,0} + \sum_{n=2}^{N-2} A_{n,0}A_{n+1,0}\right] \\ &= k\left[r\left(s+(1-s)\frac{m}{M-1}\right) + r^2 s\left(s+(1-s)\frac{m}{M-1}\right) + (N-3)r^2s^2\right] \quad (5) \\ \psi_{1,m-1}|_{\max} &= k\left[A_{1,m-1} + A_{1,m-1}A_{2,M-1} + \sum_{n=2}^{N-2} A_{n,M-1}A_{n+1,M-1}\right] \\ &= k\left[r\left(s+(1-s)\frac{m-1}{M-1}\right) + r^2\left(s+(1-s)\frac{m-1}{M-1}\right) + (N-3)r^2\right] \quad (6)\end{aligned}$$

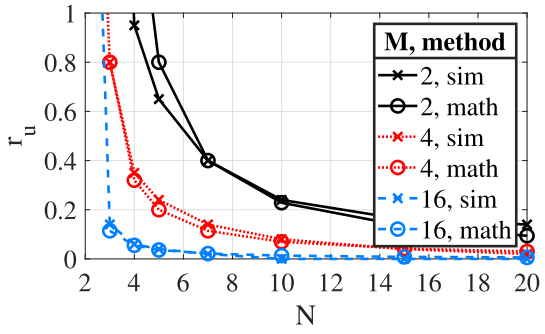

FIGURE 5. Scaled mathematical and simulated upper limit for r, with $s = 0$ and varying number of tones and modulation order of bASK-OFDM.

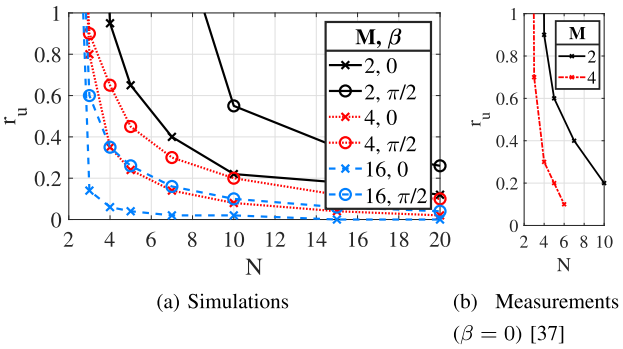

FIGURE 6. Upper limit for r (r_u), while varying N and M, for β both 0 and $\pi/2$ phase offset of the WiLO tone, with $s = 0$ for bASK-OFDM.

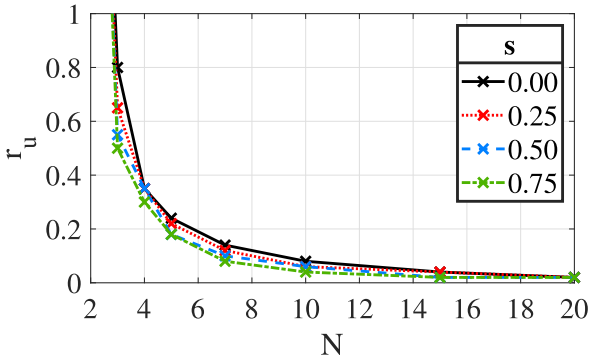

FIGURE 7. Simulation results for upper limit for r (r_u), while varying N and s, for both 0 phase offset of the constant tone, with $M = 4$ for bASK-OFDM.

useful IM_2 when more other information tones have high amplitude. This property is not captured in our model when we combine the result of (2) for multiple tone pairs. This means that, certainly for bASK with $s = 0$, where some tones have zero magnitude, k in (5) and (6) can be different. The reason that our model without accounting for this power interference results in lower r_u, is that $\psi_{1,m}|_{\min}$ is larger than calculated with (5) and $\psi_{1,m-1}|_{\max}$ is lower than calculated with (6). This is further addressed in Section V.

B. SIMULATION MODEL FOR WILO SCALING

For bASK with in-phase WiLO tone ($\beta = 0$), verifying the cluster overlap in the previous section is straightforward since all output $\psi_{n,m}$ are nearly on a line for each output tone n. However, for more general scenarios like bASK-OFDM with $\beta \neq 0$, OFDM with QAM or PSK tone modulations, or other types of information signals, this approach can not be used. Instead, for flexibility, machine learning is used to cluster and classify the received $\psi_{n,m}$ outputs. Classical symbol demodulation can be used on each tone, but results in lower r_u unless adjusted to the non-Gaussian distributed $\psi_{n,m}$ as shown in Fig. 4. Instead, a support vector machine (SVM) trained on at least 2000 OFDM symbols is used.

Fig. 6 shows the impact of varying the modulation order M, the number of tones N, and WiLO phase β on maximal amplitude of information tone r_u, while the ratio of the individual tone's minimal and maximal amplitude $s = 0$ for ASK-OFDM, using SVM-based receiver simulations and measurements. Increasing M decreases r_u since the noise margin between outputs $\psi_{n,m}$ on tone n decreases, and the information signal becomes more sensitive to interference. r_u also has to decrease with increasing N since more information tones will cause more interference. Both effects are validated by ASK-OFDM measurement results presented in [37] and shown by these simulations when for example comparing $r_u = 0.65$ when $N = 5$ and $M = 2$, and $r_u = 0.1$ when $N = 10$ and $M = 4$. This figure also shows the increase of r_u when choosing WiLO phase offset $\beta = \pi/2$ as further discussed in Section III-C. In this case the upper limit for r increases for example from $r_u = 0.2$ to $r_u = 0.55$ when $N = 10$ and $M = 2$.

When applying the bASK modulation scheme to the information tones, the ratio between minimal and maximal tone amplitude s can also be varied to ensure some minimal fixed amplitude on each tone and higher PAPR in each OFDM symbol, as is beneficial for WPT. For classical ASK $s = 0$, but when increasing s, the noise margin decreases and minimal interference increases, as can be expected from the discussion in (8). Hence, r_u decreases as shown in Fig. 7. For example, $r_u = 0.8$ decreases to $r_u = 0.5$ when the ratio of the individual tone's minimal and maximal amplitude, s is increased from $s = 0$ to $s = 0.75$, for the $N = 3$ and $M = 4$ case. For $s \approx 1$, the ASK amplitudes on the different tones are nearly the same. So, this means that the interfering intra-IM is nearly independent of the amplitudes on the other tones, and only the number of tones limits r_u as each dominant second-order intermodulation product in the baseband is impacted by similar interference. So, r_u does not automatically converge to 0 for s approaching 1. The decreasing noise margin but consistent interference for increasing s leads to a lower impact of s on r_u than intuitively expected.

C. WILO PHASE OPTIMIZATION

In the previous subsection, the WiLO amplitude A from (1) has been changed by varying r, while designing WiLO phase $\beta = 0$ or $\beta = \pi/2$. Choosing $\beta = \pi/2$ was shown to increase r_u for bASK-OFDM. The impact of the WiLO phase β is further analyzed in this section.

The motivation for the WiLO's phase offset is the fact that it is known from (2) that the phase of each intermodulation

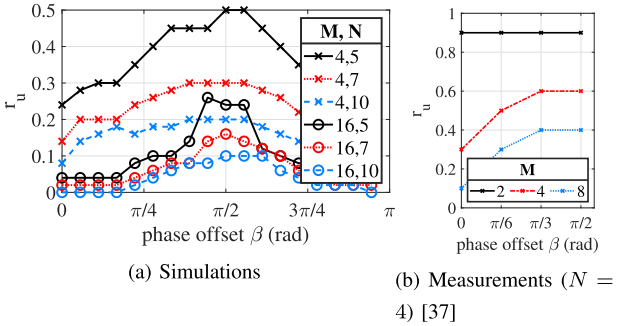

(a) Simulations

(b) Measurements ($N = 4$) [37]

FIGURE 8. Upper limit for r, r_u, while varying phase offset β, modulation order M, and number of tones N for ASK-OFDM.

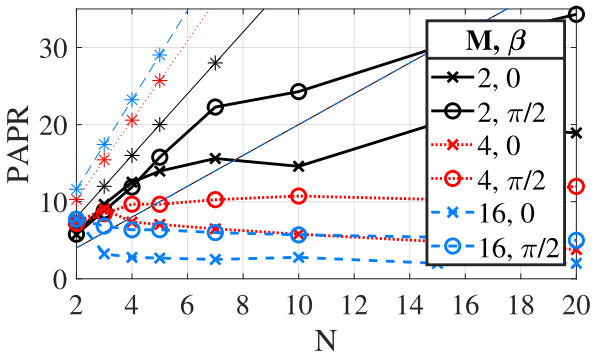

FIGURE 9. Simulated PAPR when $r = r_u$, while varying modulation order M and number of tones N for bASK-OFDM, with $s = 0$.

contribution is related to the initial phase difference between the two intermodulating tones $\phi_1 - \phi_2$. We assume that within a bASK-OFDM symbol, the information tones have phase ϕ_{inf}, and the WiLO has phase ϕ_{WiLO} at the diode input. This means that for the bASK modulated OFDM signal, where all information tones are in-phase, the intra-IM among information tones have phase $\phi_{\text{inf}} - \phi_{\text{inf}} \approx 0$. The phase of the inter-IM between each information tone and the WiLO have $\phi_{\text{WiLO}} - \phi_{\text{inf}} \approx \beta$. So, by changing β, the phaser of the inter-IM can be set orthogonal to the phaser of the interfering intra-IM. This lowers the impact of interference by other information tones since it is nearly orthogonal to the noise margin. This effect is illustrated by comparing the constellations in Fig. 2(b) with $\beta = 0$ and Fig. 4 with $\beta = \pi/2$ For bASK modulated multisine signals, Fig. 8 shows that optimally $\beta \approx \pi/2$ as expected. Measurement results from [37] confirm the beneficial impact of WiLO phase offset for ASK-OFDM.

These results show that controlling the WiLO phase offset for a collocated WiLO- and information signal transmitter can provide significant improvements. On the other hand, when the transmitters are not collocated or coordinated, Fig. 8 shows that the technique can work with any relative WiLO phase rotation.

D. WILO-ASK-OFDM PAPR

It is well known that multitone signals like classical OFDM can have high PAPR, causing extra distortion due to transmitter non-linearity. While communication research tries to minimize OFDM's PAPR, signals with high PAPR have been shown to increase the efficiency of wireless power transfer [43]. Hence, it is worth investigating how the proposed scheme changes the WiLO-OFDM signal's PAPR. The PAPR of such a bASK-OFDM signal with an in-phase WiLO is calculated using

$$\text{PAPR} = \frac{(1 + (N-1)r)^2}{\frac{1}{2} + (N-1)\frac{1}{M}\sum_{i=0}^{M-1}\frac{A_{n,m}^2}{2}}, \tag{9}$$

showing that PAPR indeed decreases with decreasing r. A higher value of r provides better power conversion efficiency for WPT. However, this is at a cost of decreased noise margin as discussed in Section II-C2. Therefore, there exists a trade-off between WPT performance and WIT performance corresponding to an optimum r. For standard ASK (with $s = 0$), (9) simplifies to:

$$\text{PAPR}_{s=0} = \frac{2(1 + (N-1)r)^2}{1 + (N-1)r^2\frac{2M-1}{6(M-1)}}, \tag{10}$$

when β is not zero, and a phase offset is applied, the expression for PAPR in (9) changes. The average power expressed in the denominator remains unchanged, while peak power decreases and the expression in the numerator changes.

The simulation results for PAPR when $r = r_u$ in Fig. 9 show that while increasing the number of tones N classically increases OFDM's PAPR, it is here counteracted by the consequential decrease of r_u. This effect is more apparent for high modulation order M. Additionally, while multitone signals classically maximize PAPR when the tones are in phase, here, the 90-degree phase offset of the strong WiLO results in a higher PAPR nevertheless as r_u increases. Compared to classical modulated N-tone OFDM (asterix), PAPR decreases, and it is also lower compared to the unmodulated N-tone multisine case (unmarked) for which PAPR $= 2N$, when M and N are not small.

It is expected that increasing r_u benefits PAPR, while phase offset β is counteractive. Simulations confirmed that as phase offset β impacts r_u, peak PAPR occurs at $0 \leq \beta \leq \pi/2$ where the two aforementioned effects optimally balance. The results for PAPR show that while low s and non-zero phase offset β result in small PAPR for classical unmodulated multisine signals, here they increase PAPR as they enable a higher r_u. This impact of s when considering $\beta = 0$ can be found mathematically by combining the upper limit of r in (8) in the equation for PAPR in (10).

The impact of $\beta = \pi/2$ for bASK was also already shown in Fig. 6 and Fig. 7 when varying s, M and N. The upper limit for r and the impact of varying β for PSK and QAM modulations is discussed next.

IV. COMPLEX OFDM

The first introduction of the proposed WiLO technique in [37] and the previous section only consider amplitude-modulated information tones. In this section, PSK and QAM

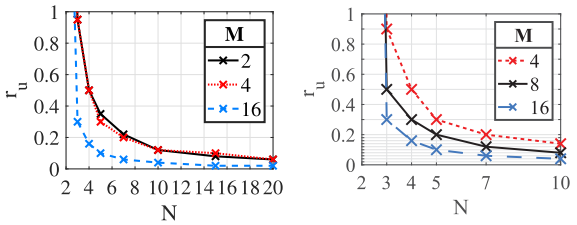

(a) Simulations (b) Measurements

FIGURE 10. Upper limit for r, for PSK modulated OFDM, with $\beta = 0$.

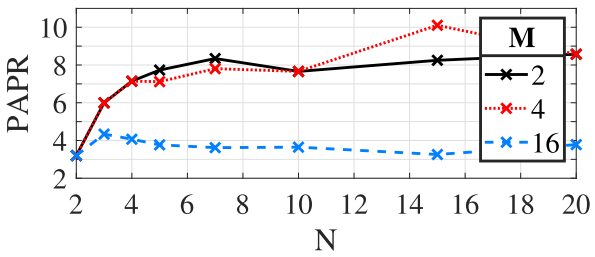

FIGURE 11. Simulated PAPR, for WiLO- PSK modulated OFDM, with $\beta = 0$.

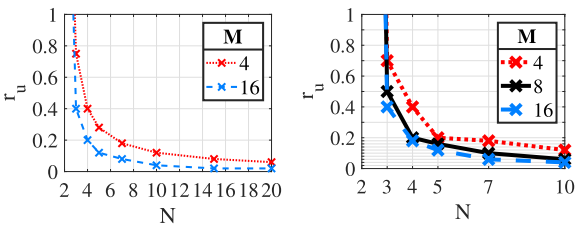

(a) Simulations (b) Measurements

FIGURE 12. Upper limit for r, for QAM modulated OFDM, with $\beta = 0$.

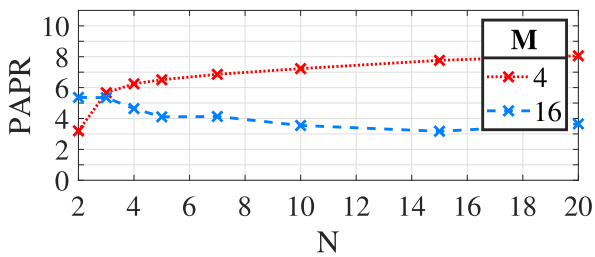

FIGURE 13. Simulated PAPR, for WiLO- QAM modulated OFDM, with $\beta = 0$.

modulation are applied to information tones, demonstrating that also phase information can be recovered. These measurements are obtained with the same setup as for ASK-OFDM in [37]. The reason that phase modulation can be recovered without LO is the phase relationship between the input tone phases and the IM_2 phase in (2).

A. PSK MODULATION

Here, PSK modulation is applied individually to every information tone while the WiLO remains constant. These PSK constellations have phases $2\pi m/M$ with $0 \leq m < M-1$ and amplitude r compared to the WiLO tone amplitude normalized to one. The receiver output is processed using SVM. The simulated and measured upper limit on r, r_u, for PSK modulated information tones with $\beta = 0$ is shown in Fig. 10. These results for PSK-OFDM show that again r_u has to decrease for higher order modulations and a higher number of tones, while also demonstrating the feasibility of receiving PSK-OFDM without LO. The upper limit r_u for PSK-OFDM is generally higher than the one found for ASK-OFDM.

Theoretically, WiLO-PSK-OFDM's PAPR is expressed by

$$\text{PAPR} = \frac{2(1+(N-1)r)^2}{1+(N-1)r^2} \tag{11}$$

which again shows that PAPR increases with r. For the extreme scenario, where r approaches the upper limit $r = r_u$, PAPR from simulations is shown in Fig. 11, which matches with using r_u from Fig. 10 in (11).

Section III-C demonstrated that changing the WiLO's phase β allowed for increasing r_u when the information tones are bASK modulated. Besides, for 2-PSK, which can be considered similar to 2-ASK modulation, simulations have shown that varying β does not improve receiver performance for PSK-OFDM significantly since the phase is modulated and the interfering intra-IMs are not aligned as was the case for ASK modulation.

B. QAM MODULATION

QAM-modulated OFDM, discussed in this subsection, can be considered as the combination of both amplitude and phase modulations covered in previous sections. The simulated and measured upper limit r_u, for QAM modulated information tones, with $\beta = 0$ is shown in Fig. 12. The results demonstrate that also for WiLO-QAM-OFDM r_u decreases for increasing M and N, while r_u is generally higher compared to ASK-OFDM and PSK-OFDM as the noise margin is larger for a QAM constellation. These simulation results for QAM-OFDM show that again r has to decrease for higher order modulations and a higher number of tones while also demonstrating the feasibility of receiving QAM-OFDM without LO. The PAPR when $r = r_u$ is shown in Fig. 13, again balancing the effect of more tones and decreasing r_u. Similar to PSK-OFDM, simulations showed that varying β does not improve receiver performance significantly since the phase is modulated and the superimposed intra-IM are not aligned as was the case for ASK modulation.

V. WILO FREQUENCY OFFSET

Currently, r is limited since the inter-IMs with the WiLO coincide with the intra-IMs among the information tones. This bounds the PCE of the system as PAPR is lower in this case. This can be avoided at the cost of bandwidth or bitrate. The frequency spacing between the WiLO and the first information tone can be increased to a larger multiple of $0.5 \times \Delta f$. This will move the useful inter-IM products to higher baseband frequencies compared to the intra-IM between information tones, as shown in Fig. 1.

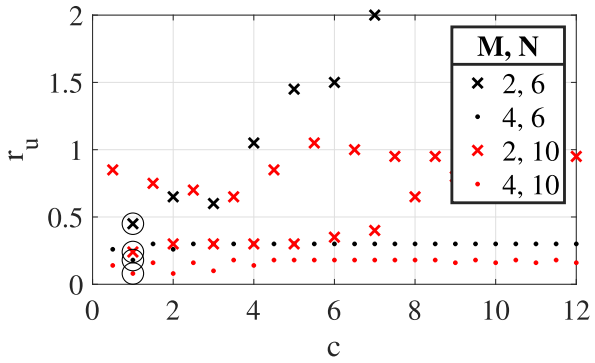

FIGURE 14. Simulated impact of frequency spacing $c\Delta f$ between the WiLO and the first tone of the OFDM spectrum on r_u, for $N = 6$ and 10, and $M = 2$ and 4.

This frequency spacing between the WiLO and the first information tone was defined as $c \times \Delta f$, with c multiples of 0.5. Fig. 14 shows the impact of increasing c on r_u, for c multiples of 0.5 between 0.5 and 12.

The results confirm that r_u increases for increasing integer c or when $c = n + 0.5$ with integer n. For the former, r_u increases for increasing integer c since the inter-IMs overlap less with the intra-IMs as can be seen in Fig. 1. The latter are located at the first $N - 1$ multiples of Δf. For non-integer c, r_u also increases as the inter-IM are located at odd multiples of $0.5\Delta f$ whereas the intra-IM are located at even multiples. This lack of overlap between inter-IM and intra-IM significantly increases r_u, as can be seen for odd c and for example the $N = 10$ and $M = 2$ case.

A. SPECTRAL EFFICIENCY

It should be noted that for $c = n + 0.5$ with integer n, OFDM bitrate decreases with 50% for fixed information signal bandwidth since the FFT's precision has to double. The case with $c = 0.5$ actually resembles ACO-OFDM from [44] for Hermitian symmetric signals in optimal communications but without the DC clipping. However, such signals reduce spectral efficiency by a factor of four. The optical communication's DCO-OFDM alternative still reduces spectral efficiency by a factor of two. For generating non-negative signals, as these optical techniques are restricted to have Hermitian symmetry, not all the sub-carriers can be used for data which affects spectral efficiency [44], [45], [46], [47]. However, our proposed WiLO-OFDM need not be Hermitian, and the signal can be complex, utilizing all subcarriers for data transmission and increasing spectral efficiency. Hence, our proposed technique outperforms optical communications' DCO-, ACO- and ADO-OFDM and is more suited for the considered low-power RF communication system.

For very large c, the technique resembles the millimeter wave signals used in heterodyne and self-homodyne receivers [48], [49], [50]. Spectral efficiency is also increased compared to millimeter-wave heterodyne and self-homodyne techniques as the constant tone can be located very close to the information spectrum. Additionally, the proposed technique allows the sharing of the WiLO tone among different information channels, as illustrated by the OFDM signal in this paper. Fig. 14 shows that r_u converges for frequency offset $c = n + 0.5$ or large c. This can be explained by power interference.

B. POWER INTERFERENCE

According to the additive second-order intermodulation interference model based on second-order additive interference from Section III-A, interference fully disappears for $c > N - 1$ as well as for non-integer c. However, this is only the case when the higher-order intermodulations and power interference are not accounted for. It is important to note that choosing $c = 0.5+n$ with integer n or choosing $c \gg N$ does not fully remove the intermodulation interference of other tones, but the upper limit r_u converges. Simulation results show for large $c \geq N$ and $M \geq 4$, that r_u converges to $1.6^{3-\log_2 M}/(N-1)$. Interestingly, such a factor of 1.6 also improved the accuracy of the mathematical model in Fig. 5. The reason for this convergence is mainly the aforementioned power interference, which is not captured by the simplified model in Section III. The strength of the created inter-IM between the WiLO and an information tone depends on how many other tones are present and their strengths as the information tone also intermodulates with those tones. So, more tones in the signal result in a weaker inter-IM output contribution. For example, consider a 4-ASK modulation on two tones with two largest tone amplitudes $a_{n,2} = 2/3r$ and $a_{n,3} = r$, and large spacing $c\Delta f$ between WiLO and the information spectrum. For tone n, the output in $\psi_{n,3}$ is smallest when all other information tones are maximal and have $a_n = a_{n,3}$, so tone amplitudes $[1, r, r]$. In this case, the intermodulation power is spread. The output $\psi_{n,2}$ for input tone n is maximal when all other tones but the WiLO are $a_n = a_{n,0} = 0$, so tone amplitudes $[1, 0, 2/3r]$. For perfect information transfer, we required having no overlap between outputs $\psi_{n,m}$ on tone n. It can be seen from this discussion that the upper limit r_u is lower for more tones, and for larger M. Choosing a minimal binary modulation order per tone $M = 2$, which implies only using $a_{n,0} = 0$ and $a_{n,1} = r$ on each tone, is very robust to power scaling as output $\psi_{n,0}$ remains zero and the $\psi_{n,1}$ is subject to scaling but can not go below 0. Modeling this scaling due to power interference is non-trivial and particularly relevant for large c where additive interference is negligible. Increasing bASK bias s does decrease the power scaling impact as all amplitudes on each of the other tones are more similar. Nevertheless, noise margin also decreases, and simulations show that this latter effect is dominant and r_u decreases compared to $s = 0$.

So, increasing WiLO frequency offset clearly increases r_u at the cost of decreasing spectral efficiency, and r_u converges. While OFDM signals with many tones and high modulation orders would lead to a very strong WiLO tone relative to the information signal, increasing WiLO offset c decreases this effect and makes the technique more practically feasible. In this way, both requirements for

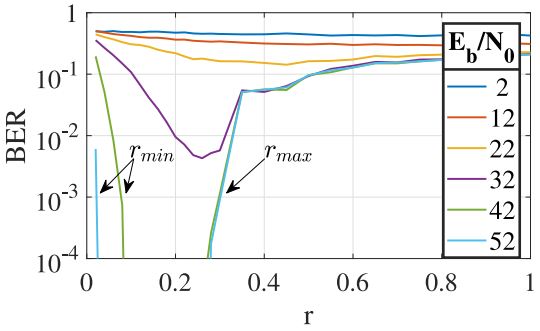

FIGURE 15. ASK-OFDM simulation results for BER when varying SNR (E_b/N_0) and r, with $\beta = \pi/2$, $M = 8$ and $N = 6$.

SWIPT, information decoding as well as power transfer can be addressed simultaneously.

VI. AWGN CHANNEL

This section analyzes two characteristics of the proposed WiLO-OFDM scheme in the presence of an AWGN channel. Firstly, the optimal signal scaling that minimizes bit error rate (BER) and maximizes throughput for certain SNR, r_{o} is determined. On the one hand, with small r the power of the information tones is very low, leading to a low information signal-to-noise power ratio. On the other hand, maximizing r leads to large information tone power but also maximal interference by the other tones, causing a large impact of the added noise as the noise margin between ψ's gets small. Hence, the optimal r, r_{o}, is somewhere in between 0 and r_{u}. Secondly, simulations demonstrate the difference in performance between classical OFDM and the proposed technique for a noisy channel, characterizing the downside of receiving such a signal with a diode instead of using a local oscillator.

A. IMPACT OF AWGN CHANNEL ON r

When increasing noise power, the range for usable r, for which BER $\leq 10^{-3}$, is defined by $r_{\min}$ and $r_{\max}$, with $0 \leq r_{\min} \leq r_{\mathrm{o}} \leq r_{\max} \leq r_{\mathrm{u}}$. The impact of noise on this usable r-range, for ASK-OFDM is shown in Fig. 15. The simulation results show that noise both increases the under limit ($r_{\min}$) and decreases the upper limit ($r_{\max}$) for r. This can be seen when adding noise ϕ to (4): $\psi_{n,m}|_{\min} - \phi_n > \psi_{n,m-1}|_{\max} + \phi_n$. $r_{\min}$ increases since for too small r, the WiLO is strong and a small SNR still has a large impact on the small information tones, so ϕ is large relative to ψ. $r_{\max}$ decreases when noise increases, since for $r = r_{\mathrm{u}}$, the noise margin is fully reduced because of intra-IM interference as shown in Fig. 2 and r has to decrease from r_{u} to cope with the channel noise so that $\psi_{n,m}|_{\min} - \psi_{n,m-1}|_{\max}$ is large enough compared to combined effect of $\phi_n + \phi_n$ over baseband outputs $\psi_{n,m}$. For high noise levels, there is no r for which information can be decoded without errors, as expected.

The region $r_{\min}$ and $r_{\max}$ for which BER $< 10^{-3}$ is shown in Fig. 16 for different modulation order M, number of tones N, and noise level with vertical dotted lines. The AWGN

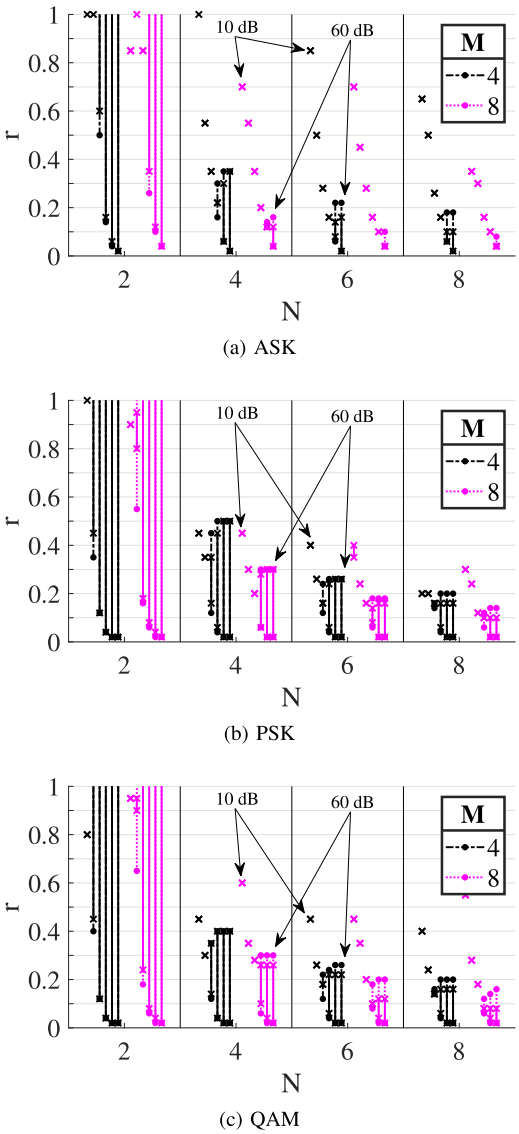

FIGURE 16. ASK (a),PSK (b) and QAM (c) simulation results for r indicating $BER < 10^{-3}$ region $r_{min} \leq r \leq r_{max}$ (dotted vertical lines with dot markers) and minimal BER region r_o (full vertical lines with cross markers), when $(N-1)E_b/N_0$ varies from 10 dB to 60 dB in steps of 10 dB, with varying N and M.

channel is applied to ASK-OFDM, PSK-OFDM, and QAM-OFDM. The optimal $r = r_{\mathrm{o}}$ for which BER is minimal (and throughput is maximal) is indicated with full vertical lines and cross markers. $r_{\min}$ and $r_{\max}$ are both indicated with a dot marker and connected with a dotted vertical line indicating BER $\leq 10^{-3}$. The results confirm that with noise, $0 \leq r_{\min}$ and $r_{\max} \leq r_{\mathrm{u}}$.

B. COMPARISON BETWEEN CLASSICAL AND WILO-OFDM

While our proposed WiLO-OFDM technique can be received without LO, some cross-tone interference is created in the receiver process, which degrades performance in the presence of noise differently compared to classical OFDM. When adding additive white Gaussian noise (AWGN) to the different WiLO-OFDM signals, simulation results show

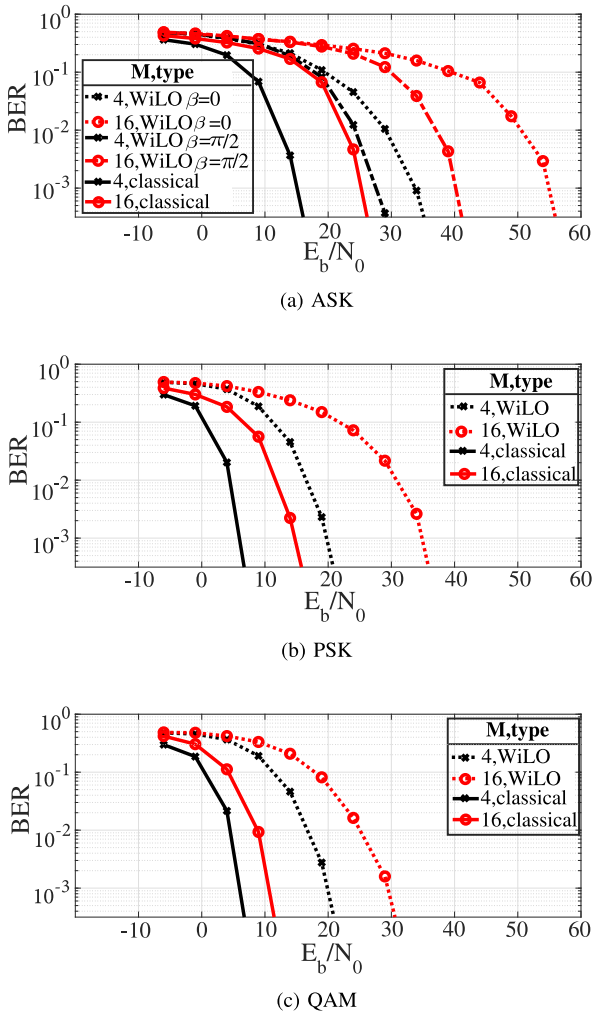

FIGURE 17. Simulated performance of the proposed ASK-WiLO-OFDM scheme with and without 90-degree phase offset, and PSK-WiLO-OFDM and QAM-WiLO-OFDM, and classical OFDM, with 4 individually modulated tones, respectively, $M = 4$ and 16, and AWGN noise, with E_b also 1/4-th of the WiLO energy.

that classical OFDM performs better than the proposed LO-less technique as expected, as shown in Fig. 17. For the WiLO technique results, r is set to r_o to get the best possible performance regarding BER for fixed N and M. The proposed bASK-OFDM signal is only functional for relatively high SNR as shown in Fig. 17(a). However, when applying the $\beta = \pi/2$ degrees WiLO phase offset, the noise performance difference significantly increases. For PSK and QAM, comparison with classical OFDM in Fig. 17(b) and Fig. 17(c) again shows that classical OFDM performs better.

The proposed technique does decrease performance with an AWGN channel and OFDM signal compared to classical OFDM systems, as expected. However, removing the LO in the receiver saves a significant amount of power, while WIT is still possible and only loses around 12 dB, regarding performance in the presence of noise. SWIPT applications, where power is also transferred, typically operate in a high SNR regime, where the proposed WiLO-OFDM scheme performs well. Therefore, this can be acceptable for SWIPT systems where energy harvesting and information transfer become equally important.

VII. OUTLOOK TOWARDS WILO SYSTEM INTEGRATION

This technique of using the WiLO tone and the receiver's non-linearity for downconversion can be combined with backscattering and energy harvesting, resulting in an energy-efficient IoT system. These three subsystems and their integration are discussed next.

1) INFORMATION DOWNCONVERSION

The received WiLO should be strong enough to respect the upper limit on r. If the WiLO transmitter is different from the information signal transmitter, worst-case path loss for the WiLO can be assumed and the WiLO transmit power can be designed accordingly. It is worth noting that simulations with a classical Bluetooth transceiver, modified with the proposed WiLO tone and diode receiver, also showed the feasibility of the technique for such a non-OFDM signal. For example, when the WiLO is located at the edge of the 2 MHz channel, the Gaussian frequency shift keying modulated information was retrievable, even with a very weak WiLO tone, as there are no other interfering frequency components. The interaction between the constant tone and Bluetooth frequency shifting tone can also be viewed as 2-tone FSK, as was proposed in [34], [39]. The WiLO tone can also be shared among Bluetooth channels, since neighboring information channels resemble the OFDM case, described in detail in this work.

2) BACKSCATTERING

Research has demonstrated backscattering on a single constant tone [8], [9]. So, depending on the backscatter receiver, the frequency difference between the WiLO and the information signal can be enlarged if interference between the backscattered signal and the original information signal at other WiLO-based sensors is minimized.

3) ENERGY HARVESTING

While sensors can harvest energy from the described signals, practical wireless power transfer, and energy harvesting are more efficient if the received waveform is deterministic with a high PAPR. As discussed in, for example, Section III, the design of the downconversion technique impacts the signal's PAPR, which should be designed accordingly to balance received information with received energy. Beamforming to overcome path loss might also be included to increase the received power level at the sensor and harvest more energy. For more efficient energy harvesting, the WiLO can be extended to multiple tones as long as the additional inter-intermodulations do not coincide, which can be controlled by varying the frequency spacing of the multitone signal. Some existing SWIPT modulation techniques, optimized to transfer both information and power, can easily be considered as special case examples of the proposed WiLO-technique [31], [34], [39], [51].

Besides designing a WiLO-modified multitone signal that enables the three aforementioned techniques simultaneously, MAC protocols can be designed to alternate between an appropriately designed information signal to allow for LO-less downconversion as discussed in this paper, or for efficient energy transfer using a classical multisine signal with uniform amplitude and phase, when appropriate frequency spacings are used. The latter can also be used for backscattering as the classic multisine signal portion is fully deterministic and constant.

VIII. CONCLUSION

This work demonstrates that modulated RF signals with high complexity, like OFDM, can be received without a local oscillator and mixer. Such a receiver saves a considerable amount of power, allowing a low power world of Internet-of-Things, where nodes might be even powered wirelessly.

Only one extra constant tone and designing its amplitude A and phase β (and frequency offset c) are required to make the signal receivable without a local oscillator. These design parameters allow to control of the intermodulations by the diode and to successfully downconvert any communication signal to the baseband with a diode. These parameters depend on the information signal. The WiLO-based downconversion is studied with a mathematical model, simulations, and experimental results. We demonstrate the optimal performance for biased ASK, PSK, and QAM modulated multisine signals for the noiseless and noisy case, both resulting in different constraints on maximal information tone amplitude r. Also, there exists a trade-off between WPT performance, i.e., PAPR, and WIT performance, i.e., BER, with respect to r. The proposed WiLO scheme has a higher bit error rate than classical OFDM for an AWGN channel as expected, resulting in a 12 dB loss, but high SNR operating conditions can be expected for close-range and possibly wirelessly powered sensor IoT applications. For future work, it is interesting and relevant to also study the technique's performance for other types of channels.

The proposed receiver technique, which allows for receiving any signal without LO, is applicable in, among others, SWIPT, mmWave, and optical receivers, where power is scarce, LOs are costly, or the system is too sensitive to LO inaccuracies as the downconverted signal is not impacted by carrier frequency offsets. The fact that the WiLO can be located at a flexible frequency that is close or further from the information spectrum allows it to be shared by multiple signals in different frequency bands. To conclude, the WiLoT enables uplink information backscattering, downlink LO-less information receiving, and energy harvesting, proving itself very promising for IoT applications.

REFERENCES

[1] T. D. Ponnimbaduge Perera, D. N. K. Jayakody, S. K. Sharma, S. Chatzinotas, and J. Li, "Simultaneous wireless information and power transfer (SWIPT): Recent advances and future challenges," *IEEE Commun. Surveys Tuts.*, vol. 20, no. 1, pp. 264–302, 1st Quart., 2018.

[2] Q. Yu, D. He, Z. Lu, and H. Wang, "SSK-based PSK-LoRa modulation for IoT communications," *IEEE Open J. Commun. Soc.*, vol. 4, pp. 1487–1498, 2023.

[3] Y.-H. Liu et al., "A 1.9nJ/b 2.4GHz multistandard (Bluetooth low energy/Zigbee/IEEE802.15.6) transceiver for personal/body-area networks," in *IEEE Int. Solid-State Circuits Conf. Tech. Dig.*, 2013, pp. 446–447.

[4] K. Philips, "Ultra low power short range radios: Covering the last mile of the IoT," in *Proc. 40th Eur. Solid State Circuits Conf. (ESSCIRC)*, 2014, pp. 51–58.

[5] X. Zhou, R. Zhang, and C. K. Ho, "Wireless information and power transfer: Architecture design and rate-energy tradeoff," *IEEE Commun. Lett.*, vol. 61, no. 11, pp. 4754–4767, Nov. 2013.

[6] C. Pérez-Penichet, C. Noda, A. Varshney, and T. Voigt, "Battery-free 802.15.4 receiver," in *Proc. 17th ACM/IEEE Int. Conf. Inf. Process. Sens. Netw. (IPSN)*, 2018, pp. 164–175.

[7] D. Kim, H. Lee, K. Kim, and J. Lee, "Dual amplitude shift keying with double half-wave rectifier for SWIPT," *IEEE Wireless Commun. Lett.*, vol. 8, no. 4, pp. 1020–1023, Aug. 2019.

[8] U. S. Toro, K. Wu, and V. C. M. Leung, "Backscatter wireless communications and sensing in green Internet of Things," *IEEE Trans. Green Commun. Netw.*, vol. 6, no. 1, pp. 37–55, Mar. 2022.

[9] C. Xu, L. Yang, and P. Zhang, "Practical backscatter communication systems for battery-free Internet of Things: A tutorial and survey of recent research," *IEEE Signal Process. Mag.*, vol. 35, no. 5, pp. 16–27, Sep. 2018.

[10] R. Correia and N. B. Carvalho, "Design of high order modulation backscatter wireless sensor for passive IoT solutions," in *Proc. IEEE Wireless Power Transf. Conf. (WPTC)*, 2016, pp. 1–3.

[11] D. Belo, R. Correia, P. Pinho, and N. B. Carvalho, "Enabling a constant and efficient flow of wireless energy for IoT sensors," in *Proc. IEEE MTT-S Int. Microw. Symp. (IMS)*, 2017, pp. 1342–1344.

[12] S. Thomas and M. S. Reynolds, "QAM backscatter for passive UHF RFID tags," in *Proc. IEEE Int. Conf. RFID*, 2010, pp. 210–214.

[13] B. Gu, D. Li, H. Ding, G. Wang, and C. Tellambura, "Breaking the interference and fading gridlock in backscatter communications: State-of-the-art, design challenges, and future directions," *IEEE Commun. Surveys Tuts.*, early access, Jul. 31, 2024, doi: 10.1109/COMST.2024.3436082.

[14] Y. Guo, C. Skouroumounis, and I. Krikidis, "Joint information and energy transfer of SWIPT-enabled mobile users in wireless networks," *IEEE Trans. Green Commun. Netw.*, vol. 6, no. 2, pp. 1141–1156, Jun. 2022.

[15] A. Olutayo, Y. Dong, J. Cheng, J. F. Holzman, and V. C. M. Leung, "Performance of wireless powered communication systems over Beaulieu-Xie channels with nonlinear energy harvesters," *IEEE Open J. Commun. Soc.*, vol. 4, pp. 456–463, 2023.

[16] M. R. Camana, C. E. Garcia, and I. Koo, "Rate-splitting multiple access in a MISO SWIPT system assisted by an intelligent reflecting surface," *IEEE Trans. Green Commun. Netw.*, vol. 6, no. 4, pp. 2084–2099, Dec. 2022.

[17] C. R. Valenta and G. D. Durgin, "Harvesting wireless power: Survey of energy-harvester conversion efficiency in far-field, wireless power transfer systems," *IEEE Microw. Mag.*, vol. 15, no. 4, pp. 108–120, Jun. 2014.

[18] A. Collado and A. Georgiadis, "Optimal waveforms for efficient wireless power transmission," *IEEE Microw. Compon. Lett.*, vol. 24, no. 5, pp. 354–356, May 2014.

[19] B. Clerckx, R. Zhang, R. Schober, D. W. K. Ng, D. I. Kim, and H. V. Poor, "Fundamentals of wireless information and power transfer: From RF energy harvester models to signal and system designs," *IEEE J. Sel. Areas Commun.*, vol. 37, no. 1, pp. 4–33, Jan. 2019.

[20] J. Kim and B. Clerckx, "Wireless information and power transfer for IoT: Pulse position modulation, integrated receiver, and experimental validation," *IEEE Internet Things J.*, vol. 9, no. 14, pp. 12378–12394, Jul. 2022.

[21] B. Clerckx, "Wireless information and power transfer: Nonlinearity, waveform design, and rate-energy tradeoff," *IEEE Trans. Signal Process.*, vol. 66, no. 4, pp. 847–862, Feb. 2018.

[22] P. Dhull, A. P. Guevara, M. Ansari, S. Pollin, N. Shariati, and D. Schreurs, "Internet of Things networks: Enabling simultaneous wireless information and power transfer," *IEEE Microw. Mag.*, vol. 23, no. 3, pp. 39–54, Mar. 2022.

[23] A. Boaventura, N. B. Carvalho, and A. Georgiadis, "The impact of multi-sine tone separation on RF-DC efficiency," in *Proc. Asia-Pacific Microw. Conf.*, Nov. 2014, pp. 606–609.
[24] D. Alqahtani, Y. Chen, W. Feng, and M.-S. Alouini, "A new non-linear joint model for RF energy harvesters in wireless networks," *IEEE Trans. Green Commun. Netw.*, vol. 5, no. 2, pp. 895–907, Jun. 2021.
[25] L. Yao, G. Dolmans, and J. Romme, "Optimal operation of RF energy rectifiers by adaptive number of frequency selection using multisine excitation," in *Proc. 51st Eur. Microw. Conf. (EuMC)*, 2022, pp. 833–836.
[26] N. Decarli, M. Del Prete, D. Masotti, D. Dardari, and A. Costanzo, "High-accuracy localization of passive tags with multisine excitations," *IEEE Trans. Microw. Theory Techn.*, vol. 66, no. 12, pp. 5894–5908, Dec. 2018.
[27] S. Maas, "Two-tone intermodulation in diode mixers," *IEEE Trans. Microw. Theory Techn.*, vol. 35, no. 3, pp. 307–314, Mar. 1987.
[28] R. F. Buckley and R. W. Heath, "Selective OFDM transmission for simultaneous wireless information and power transfer," in *Proc. IEEE Global Commun. Conf. (GLOBECOM)*, 2019, pp. 1–6.
[29] R. F. Buckley and R. Heath, "System and design for selective OFDM SWIPT transmission," *IEEE Trans. Green Commun. Netw.*, vol. 5, no. 1, pp. 335–347, Mar. 2021.
[30] S. Claessens, N. Pan, M. Rajabi, D. Schreurs, and S. Pollin, "Enhanced biased ASK modulation performance for SWIPT with AWGN channel and dual-purpose hardware," *IEEE Trans. Microw. Theory Techn.*, vol. 66, no. 7, pp. 3478–3486, Jul. 2018.
[31] M. Rajabi, N. Pan, S. Claessens, S. Pollin, and D. Schreurs, "Modulation techniques for simultaneous wireless information and power transfer with an integrated rectifier-receiver," *IEEE Trans. Microw. Theory Techn.*, vol. 66, no. 5, pp. 2373–2385, May 2018.
[32] D. I. Kim, J. H. Moon, and J. J. Park, "New SWIPT using PAPR: How it works," *IEEE Wireless Commun. Lett.*, vol. 5, no. 6, pp. 672–675, Dec. 2016.
[33] C. Im, J. Lee, and C. Lee, "A multi-tone amplitude modulation scheme for wireless information and power transfer," *IEEE Trans. Veh. Technol.*, vol. 69, no. 1, pp. 1147–1151, Jan. 2020.
[34] S. Claessens, N. Pan, D. Schreurs, and S. Pollin, "Multitone FSK modulation for SWIPT," *IEEE Trans. Microw. Theory Techn.*, vol. 67, no. 5, pp. 1665–1674, May 2019.
[35] P. Dhull, D. Schreurs, G. Paolini, A. Costanzo, M. Abolhasan, and N. Shariati, "Multitone PSK modulation design for simultaneous wireless information and power transfer," *IEEE Trans. Microw. Theory Techn.*, vol. 72, no. 1, pp. 446–460, Jan. 2024.
[36] J. F. Ensworth, A. T. Hoang, and M. S. Reynolds, "A low power 2.4 GHz superheterodyne receiver architecture with external LO for wirelessly powered backscatter tags and sensors," in *Proc. IEEE Int. Conf. RFID*, 2017, pp. 149–154.
[37] S. Claessens, Y. T. Chang, D. Schreurs, and S. Pollin, "Receiving ASK-OFDM in low power SWIPT nodes without local oscillators," in *Proc. IEEE Wireless Power Transf. Conf.*, Jun. 2019, pp. 1–5.
[38] Y. T. Chang, S. Claessens, D. Schreurs, and S. Pollin, "A wideband efficient rectifier design for SWIPT," in *Proc. IEEE Wireless Power Transf. Conf.*, Jun. 2019, pp. 1–5.
[39] S. Claessens, D. Schreurs, and S. Pollin, "Two-tone FSK modulation for SWIPT," in *Proc. IEEE Wireless Power Transf. Conf.*, Jun. 2018, pp. 1–4.
[40] Q. Wu, Y. Zhao, Q. Fan, P. Fan, J. Wang, and C. Zhang, "Mobility-aware cooperative caching in vehicular edge computing based on asynchronous federated and deep reinforcement learning," *IEEE J. Sel. Topics Signal Process.*, vol. 17, no. 1, pp. 66–81, Jan. 2023.
[41] Q. Wu, S. Shi, Z. Wan, Q. Fan, P. Fan, and C. Zhang, "Towards V2I age-aware fairness access: A DQN based intelligent vehicular node training and test method," *Chin. J. Electron.*, vol. 32, no. 6, pp. 1230–1244, Nov. 2023.
[42] S. Claessens, D. Schreurs, and S. Pollin, "SWIPT with biased ASK modulation and dual-purpose hardware," in *Proc. IEEE Wireless Power Transf. Conf.*, May 2017, pp. 1–4.
[43] A. S. Boaventura and N. B. Carvalho, "Maximizing DC power in energy harvesting circuits using multisine excitation," in *Proc. IEEE MTT-S Int. Microw. Symp.*, Jun. 2011, pp. 1–4.
[44] J. Armstrong and A. Lowery, "Power efficient optical OFDM," *Electron. Lett.*, vol. 42, no. 6, p. 370, 2006.
[45] J. Kahn and J. Barry, "Wireless infrared communications," *Proc. IEEE*, vol. 85, no. 2, pp. 265–298, Aug. 2002.
[46] S. D. Dissanayake, K. Panta, and J. Armstrong, "A novel technique to simultaneously transmit ACO-OFDM and DCO-OFDM in IM/DD systems," in *Proc. IEEE GLOBECOM Workshops (GC Wkshps)*, 2011, pp. 782–786.
[47] S. D. Dissanayake and J. Armstrong, "Comparison of ACO-OFDM, DCO-OFDM and ADO-OFDM in IM/DD systems," *J. Lightw. Technol.*, vol. 31, no. 7, pp. 1063–1072, Apr. 1, 2013.
[48] Y. Shoji, M. Nagatsuka, K. Hamaguchi, and H. Ogawa, "60 GHz band 64 QAM/OFDM terrestrial digital broadcasting signal transmission by using millimeter-wave self-heterodyne system," *IEEE Trans. Broadcast.*, vol. 47, no. 3, pp. 218–227, Sep. 2001.
[49] A. Islam, M. Bakaul, A. Nirmalathas, and G. E. Town, "Millimeter-wave radio-over-fiber system based on heterodyned unlocked light sources and self-homodyned RF receiver," *IEEE Photon. Technol. Lett.*, vol. 23, no. 8, pp. 459–461, Apr. 15, 2011.
[50] A. R. Islam, M. Bakaul, A. Nirmalathas, and G. E. Town, "Simplification of millimeter-wave radio-over-fiber system employing heterodyning of uncorrelated optical carriers and self-homodyning of RF signal at the receiver," *Opt. Express*, vol. 20, no. 5, p. 5707, 2012.
[51] M. Rajabi, S. Pollin, and D. Schreurs, "Hybrid rectifier-receiver node," in *Proc. IEEE MTT-S Int. Microw. Symp.*, Jun. 2017, pp. 1038–1041.

STEVEN CLAESSENS received the B.Sc. and M.Sc. degrees in electrical engineering and the Ph.D. degree in simultaneous wireless information and power transfer, including waveform design, backscattering, and massive MIMO processing from KU Leuven, Belgium, in 2014, 2016, and 2020, respectively. He currently works in industry on SDR based satellite communication systems, enabling wideband signals, and AI processing.

PRERNA DHULL (Graduate Student Member, IEEE) received the M.Tech. degree in electronics and communication engineering (communication systems) from the Indian Institute of Technology Roorkee, Roorkee, India, in 2017. She is currently pursuing the double Ph.D. degree in electronics, RF, and communication technologies with KU Leuven, Leuven, Belgium, and the University of Technology Sydney, Sydney, NSW, Australia.

Her research interests include simultaneous wireless information and power transfer systems, waveform design, wireless power transfer, energy harvesting, and self-sustainable networks. She is a recipient of the University of Technology Sydney Presidential Scholarship, International Research Scholarship, GRS Publication Fund, and Thesis Completion Support Grant for her Ph.D.

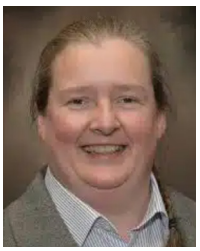

DOMINIQUE SCHREURS (Fellow, IEEE) received the M.Sc. and Ph.D. degrees in electronic engineering from KU Leuven, Leuven, Belgium, in 1992 and 1997, respectively.

She was a Postdoctoral Fellow and a Visiting Scientist with Agilent Technologies, Santa Clara, CA, USA; ETH Zürich, Zürich, Switzerland; and the National Institute of Standards and Technology, Boulder, CO, USA. She is currently a Full Professor with KU Leuven. Her research interests include microwave/mmWave metrology, device and circuit modeling, and subsystem design for wireless and biomedical applications.

Prof. Schreurs was the President for the Microwave Theory and Technology Society (MTT-S) from 2018 to 2019. She has been on IEEE MTT-S AdCom since 2009 in multiple roles. She was a Distinguished Microwave Lecturer from 2012 to 2014. She assumed the position of an Editor-in-Chief of the IEEE TRANSACTIONS ON MICROWAVE THEORY AND TECHNIQUES from 2014 to 2016. She initiated the IEEE Women in Microwaves (WiM) Event at the European Microwave Week in 2008 and has been acting as an Advisor for WiM Events. She was the Technical Program Committee Co-Chair of the International Microwave Symposium in 2023 and the Conference Chair of International Microwave Biomedical Conference in 2023. She is also the Past President of the ARFTG Organization and was involved in multiple ARFTG conferences as a Conference Chair and the TPC Chair.

SOFIE POLLIN (Senior Member, IEEE) received the Ph.D. degree (Hons.) from Katholieke Universiteit Leuven, Leuven, Belgium, in 2006. From 2006 to 2008, she continued her research on wireless communication, energy-efficient networks, cross-layer design, coexistence, and cognitive radio with the University of California at Berkeley, Berkeley, CA, USA. In 2008, she joined the Green Radio Team, Imec, as a Principal Scientist. She is currently a Professor with the Electrical Engineering Department, KU Leuven. Her research interests include networked systems that require networks that are ever more dense, heterogeneous, battery-powered, and spectrum constrained. She is a BAEF and Marie Curie Fellow.